

# Comparative Study on the Microstructure Evaluation of Al-Mg (Er5356) Aluminum Alloy for Aircraft Wing Stiffener Fabricated By Wire Arc Additive Manufacturing

Manikandan N<sup>1\*</sup>, Dr. G. Swaminathan<sup>2</sup>

<sup>1</sup>Research Scholar, Department of Mechanical Engineering, SRM Institute of Science and Technology, Ramapuram,

<sup>2</sup>Assistant Professor, Department of Mechanical Engineering, SRM Institute of Science and Technology, Ramapuram,

## \*Corresponding author

Manikandan N, Research Scholar, Department of Mechanical Engineering, SRM Institute of Science and Technology, Ramapuram.

Submitted: 28 Mar 2022; Accepted: 13 Apr 2023; Published: 19 Apr 2023

**Citation:** Manikandan, N., Swaminathan, G. (2023). Comparative Study on the Microstructure Evaluation of Al-Mg (Er5356) Aluminum Alloy for Aircraft Wing Stiffener Fabricated By Wire Arc Additive Manufacturing. *Petro Chem Indus Intern*, 6(2), 64 -74.

## Abstract

Wire + Arc additive manufacturing (WAAM) is a type of additive manufacturing process in which layer upon layer is added to form a closely welded component. In this study, Gas Metal Arc Welding - Pulse (GMAW-P) and Gas Metal Arc Welding - Double Pulse (GMAW-DP) methods were used to manufacture the components with 5356 Aluminum alloy. Microstructures of the GMAW-P and GMAW-DP were observed and compared, the results show that the bead formation, Structure, formability and continuity appeared to be better on the GMAW-DP welding when compared to GMAW-P. The pore formations were found in larger numbers in GMAW-P than GMAW-DP. Due to the presence of a larger number of pores in GMAW-P, it is weaker than GMAW-DP.

**Keywords:** WAAM, GMAW, Aluminium, Pulse Welding, Double Pulse Welding, Microstructures

## Introduction

Additive manufacturing is a process of manufacturing in which a structure is produced by adding layer upon layer. Wire + Arc Additive Manufacturing is a process that uses wire as feedstock. Heat sources that are used: GMAW - Gas metal Arc welding, GTAW - Gas Tungsten Arc Welding and PAW - plasma arc welding. Usage of Wire + Arc Additive Manufacturing helps us in manufacturing customized components with complex geometrical structure at the same time we can reduce machining cost, time and material Wastage drastically i.e. The Buy to Fly ratio (BTF) is less compared to other AM processes. As Wire arc additive manufacturing uses 6-axis robots, it has no dimensional constraints theoretically. Solidification cracking adds complexity in welding of aluminium which is greatly related with the alloy composition. The integration of materials and manufacturing process to produce defect-free and structurally-sound deposited parts remain a crucial effort into the future. Aviation components are expensive, usually titanium, aluminium and steel alloys are used in aircrafts, since manufacturing processes involving titanium should be carried out in Vacuum or Argon gas environments. Other alloys are not only expensive, the material lost during the machining of the component is up to 85%. Instead, an alternate material with which we will be able to reduce the

production cost and time, at the same time the material does not alter the properties of the component can be used. So Al-Mg alloy (Al 5356) is used which has very good formability making the manufacturing process easier. Aircraft wing stiffener is a system of parts in the wing interacting with each other as they are acted upon by combinations of pressures and bending loads. These are secondary plates which are usually attached to beam webs or flanges of the aircraft to stiffen them against the plane of deformation. Stiffeners resist bending and axial loads along with skin and divide the skin into small panels which increases the buckling under compression and failure stress. The stiffener plate will be fabricated and samples will be taken from the plate and tested for microstructures.

## Robot Used for Fabrication of the Component

The robot we use in this process is a Japanese made robot from YASKAWA Electric Corporation. Yaskawa uses INFORM and INFORM II for programming the robot. The robot uses AC current and the Robot arm (Fig. 2) can move at a speed of 30 cm /min. The Yaskawa AR 1440 YRC 1000 has 6 axes namely S, L, U, R, B, T. The movement of the robot in the axes is assigned and monitored using cartesian coordinates.



**Figure:1** Robot arm

This has a reach of 2511mm vertically and 1440 mm horizontally and has a payload of 12 kg. This is controlled using a YRC 1000 Controller also called a pendant. It has a 50 mm thru-hole to reduce cable interference and wear. An enhanced feeder mounting area on the arm reduces equipment obstruction.

### Shielding Gas

The primary purpose of shielding gas is to prevent exposure of the molten weld pool to oxygen, nitrogen and hydrogen contained in the air atmosphere. The reaction of these elements with the weld pool can create a variety of problems, including porosity (holes within the weld bead) and excessive spatter. Argon is used for shielding during fabrication. Pure argon is the most popular shielding gas. It is often used for both gas metal arc and gas tungsten arc welding of aluminum. Argon gas has a flow rate of 18L/min with a regulator pressure of 50 kg /cm<sup>2</sup>.

### Hot Start

Hot start is a feature that pumps up the amperage for a short time when you start the arc. Higher amperage helps to start the arc easier without sticking the electrode to the base metal. The hot start function allows the metals to fuse together easier at the very beginning of the weld in order for it to continue to go well.

### Crater Fill

Crater fill is just a lower voltage and wire speed setting that automatically kicks in at the end of the weld after you release the trigger. It is set with standard values or you can change the values to suit your needs.

### Power Source

The power source for the action of the robot and changes in the constraint are done through this A7 MIG POWER SOURCE

450 from KEMPPPI INDIA PVT LIMITED (Fig. 3). The current range ranges from 20 - 450 A and voltage ranges from 12 - 46V.



**Figure 2:** Power Source

### Fine Tuning

Voltage fine-tuning is a trial and error process. It's checked by inspecting the bead for deficiencies.

### Wire Feeder

A wire feeder is used to feed the material to the robot. A7 MIG WIRE FEEDER 25-ih-eur is used. A wire feeder has 4 rollers and the wire runs between them, in this way the wire is fed and the rollers straighten the wire.

### Design

3D design for aircraft wing stiffener plate is designed using Aluminium alloy 5356 as raw material. With one fixed plane, equivalent elastic stress, equivalent elastic strain and total deformation are analyses.

Click an object. Double-click to select an edge. Use. Triple-click to select a solid.

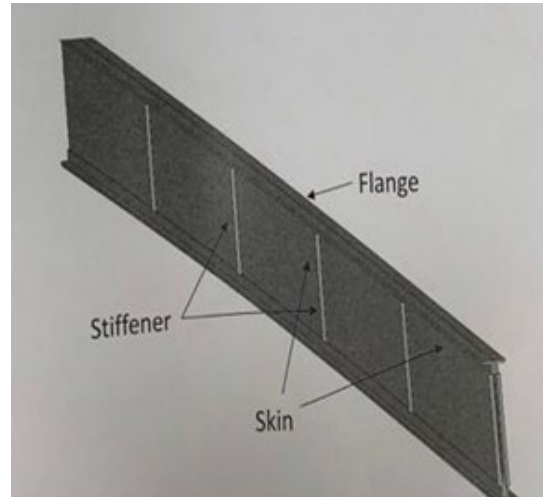
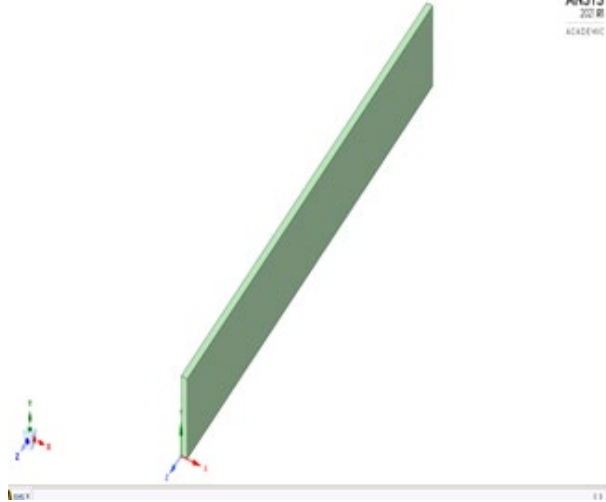


**Figure 3:** Design of Aircraft wing stiffener plate - The dimension of the wing stiffener plate is made to be 250mm\*2mm\*15mm.

### Fabrication of Sample

The base plate is chosen in such a way that the plate is able to withstand the heat. Aluminium 6061 alloy is used as base plate for the fabrication. This base plate has a thickness of 16 mm. The base plate material contains 97.9% of Aluminium (Al), 1% of Magnesium (Mg), 0.60% of Silicon (Si), 0.28% of Copper (Cu) and 0.20% of Chromium (Cr). It has a density of 2.7 g/cm and a melting point of 588°C. The aluminium wire Al5356 used for welding has a thickness of 1.2mm. The alloy consists of 93-95% of Aluminium(Al), 4-5% of Magnesium(Mg), 0.10% of Copper(Cu), 0.05-0.20% of Manganese(Mn), 0.10% of Zinc(Zn), 0.05-0.20% of Chromium(Cr), 0.06-0.20% of Titanium(Ti), 0.25% of Silicon(Si) and 0.40% of Iron(Fe).

The current, voltage and holding time can be set. Holding time is the cooling time between deposition of consecutive layers. There is a difference in unit input between the first two layers and the rest of the layers in order to set a stable and adequate base layer. The first two layers have high voltage, current and wire feed speed. The feeding torch is set. When the input for movement is provided, the torch starts to run through the way

while the molten metal is getting deposited on the base plate and stops at the end till the holding time is over. During the holding time, the temperature of the layer comes down and the layer is cleaned after formation. After the holding time it again starts the cycle from where it stops and this processes until requirement. The dimensions are measured in between the formation of each layer.

### Sample Fabricated Using Pulse Welding

Pulse or Pulse MIG welding is a method of WAAM in which a solid wire is heated and fed onto the base plate from a welding torch, to form a wall by depositing layer upon layer by pulsing the current. A 5-minute cooldown time should be given after deposition of each and every layer to avoid overheating and disintegration of the component. 12 layers are deposited one upon another to obtain a height of 30 mm and the length of the wall remains the same which is 140 mm. The thickness of the wall changes in each and every layer and height of the component differ in different parts. Voltage = 20 V, Current = 126A, Wire feed speed =8m/min. The change in thickness and height of the consecutive layers is shown in the figures. (Fig. 4 - 14).



**Figure 4:** Layer 1



**Figure 5:** Layer 3



**Figure 6:** Layer 5



Fig. 7 Layer 8



Fig. 8 Layer 10

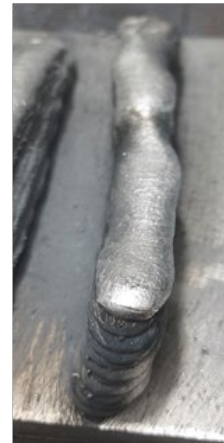
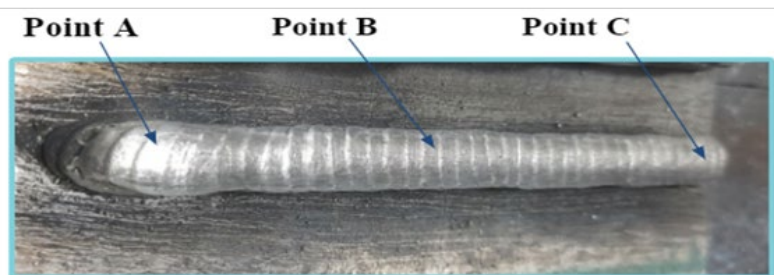


Fig. 9 Layer



**Figure 10:** Different thickness and height at the left end (POINT A), right end (POINT C) and middle part (POINT B) of the layers are shown.

After deposition of every layer, the wall thickness, height of the welded layer at both the ends and middle are observed and noted as below (TABLE 1)

Graphs are plotted between layers and their respective heights (Fig. 11) and between layers and respective widths (Fig. 12) in pulse welding.

**TABLE 1-THICKNESS AND HEIGHT LAYER BY LAYER - PULSE**

Layer		Height at Point A (mm)	Height in The Middle (mm)	Height at The Other End (mm)
Layer 1	8.16	5.08	4.50	4.37
Layer 2	10.39	7.75	6.83	6.59
Layer 3	12.36	9.92	9.32	8.83
Layer 4	12.75	12.07	11.26	10.54
Layer 5	13.66	15.25	12.76	12.63
Layer 6	14.14	18.30	15.81	14.78
Layer 7	14.34	21.36	18.28	17.18
Layer 8	14.45	23.58	19.92	19.16
Layer 9	14.81	26.41	22.78	21.13
Layer 10	14.53	28.88	24.57	22.90
Layer 11	14.43	31.24	27.00	25.50
Layer 12	14.98	33.30	29.52	25.80



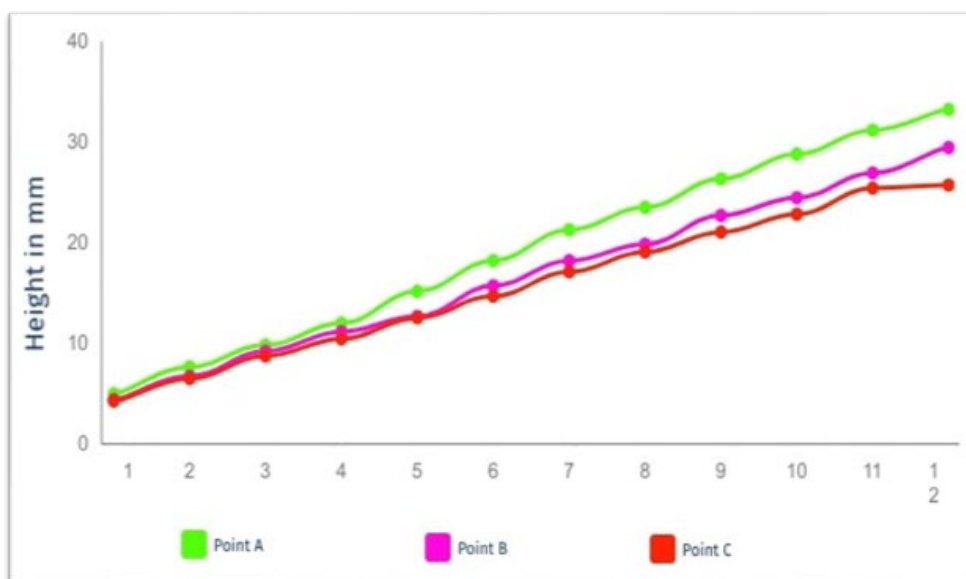


**Figure 11:** Graph is plotted between layers and their respective heights in pulse welding.

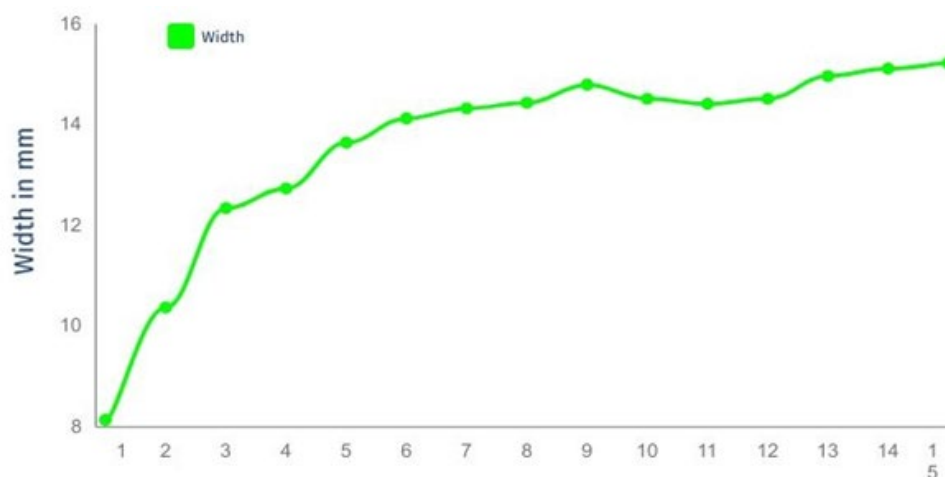


**Figure 12:** Graph is plotted between layers and their respective widths in pulse welding.

**TABLE 2 - CURRENT AND VOLTAGE FOR EACH LAYER - PULSE**

Layer	Current (A)	Voltage (V)
Layer 1	128	19.7
Layer 2	128	19.7
Layer 3	127	20.0
Layer 4	128	19.7
Layer 5	130	19.5
Layer 6	125	20.3
Layer 7	125	20.4
Layer 8	127	20.1
Layer 9	126	20.1
Layer 10	130	19.5
Layer 11	126	20.2
Layer 12	127	19.9

Graphs are plotted between layers and their respective input current in ampere in pulse welding (Fig. 13) and between layers and their respective input voltage in volt in pulse welding (Fig. 14).

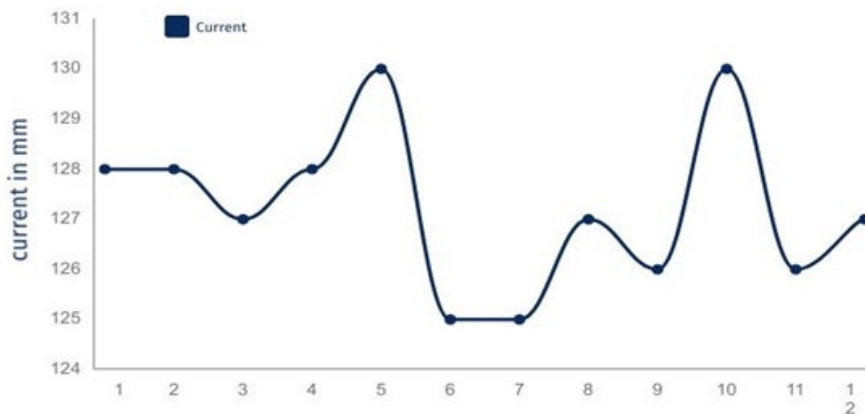


**Figure 13:** Graph is plotted between layers and their respective input current in ampere in pulse welding.

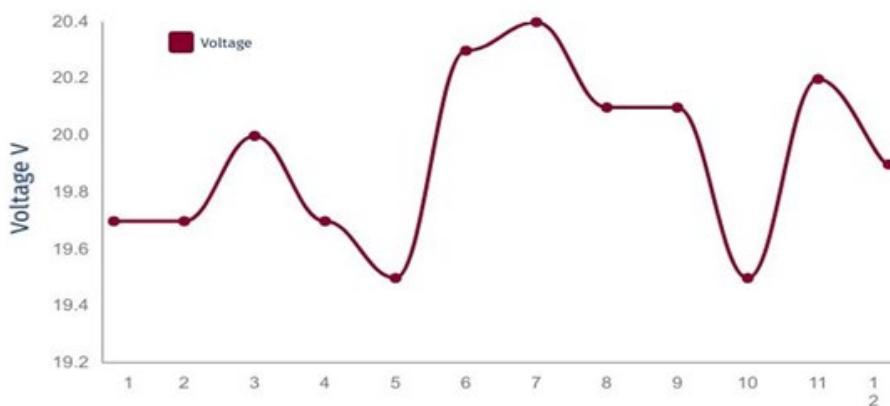


**Figure 14:** Graph is plotted between layers and their respective input voltage in volt in pulse welding.

#### Sample Fabricated Using Double Pulse Welding

Double pulse welding is a method of WAAM in which a solid wire heated and fed onto the base plate from a welding torch, to form a wall by depositing layer upon layer, by pulsing the current in two separate levels which are controlled independently. The deposition of layers is done from alternative ends for every layer. A 5-minute cooldown time should be given after deposition of each and every layer to avoid overheating and disintegration

of the component. 14 layers are deposited one upon another to obtain a height of 30 mm and the length of the wall remains the same which is 140 mm. The thickness of the wall changes in each and every layer and height of the component differ in different parts. The increase in thickness and height can be observed in the (Fig. 15- 21). Voltage = 19.2 V, Current = 112 A, Wire Feed Speed = 8m /min



**Figure 15:** Layer 1



**Figure 16:** Layer 3



**Figure 17:** Layer 5

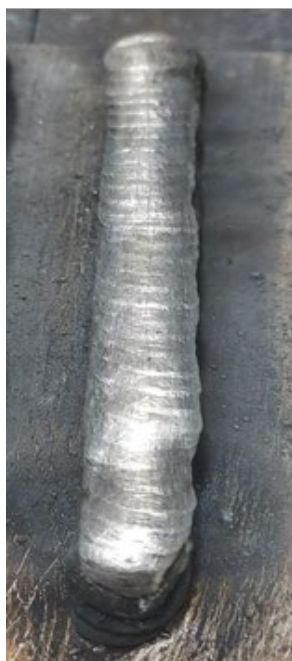


Fig 18 Layer 8



Fig. 19 Layer 11

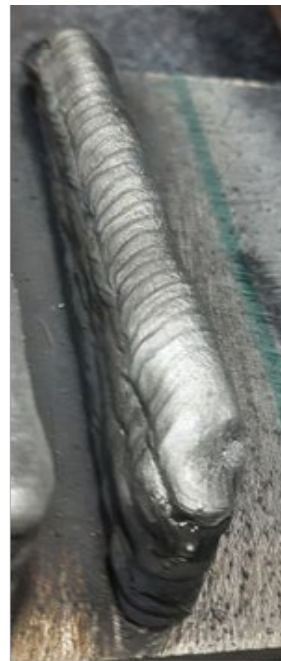
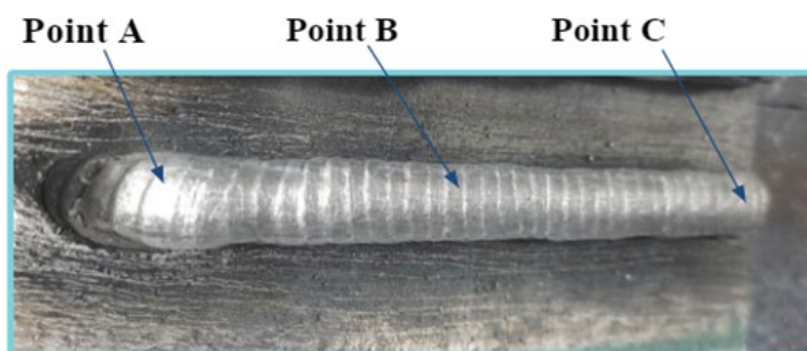


Fig. 20 Layer 14



**Figure 21:** Different thickness and height at the left end(A), right end(C) and middle part(B) of the layers are shown.

**TABLE 3-THICKNESS AND HEIGHT LAYER BY LAYER FOR DOUBLE PULSE**

Layer	Wall Thickness (mm)	Height at The One End (mm)	Height in The Middle (mm)	Height at The Other End (mm)
Layer 1	8.05	5.30	4.42	4.07
Layer 2	9.42	6.50	6.54	7.33
Layer 3	11.75	9.11	8.35	8.79
Layer 4	12.02	10.70	10.20	12.12
Layer 5	12.71	13.10	12.27	13.13
Layer 6	13.57	15.53	14.56	16.07
Layer 7	13.32	16.55	16.57	17.57
Layer 8	14.19	18.18	19.21	20.06
Layer 9	14.63	20.45	21.37	21.51
Layer 10	15.31	22.76	23.02	23.16
Layer 11	15.36	24.87	23.68	26.05
Layer 12	15.81	27.05	27.57	27.59
Layer 13	15.28	30.75	30.20	30.01
Layer 14	14.42	32.52	32.09	32.13

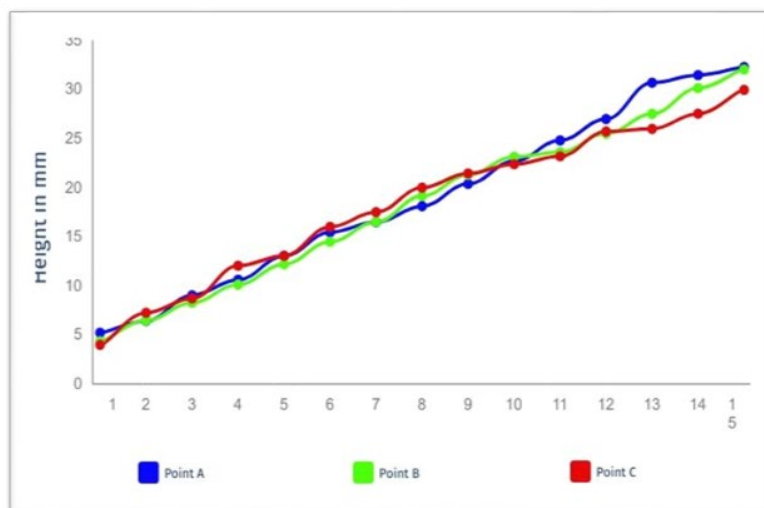


**Figure 22:** Graph is plotted between layers and their respective heights in Double Pulse

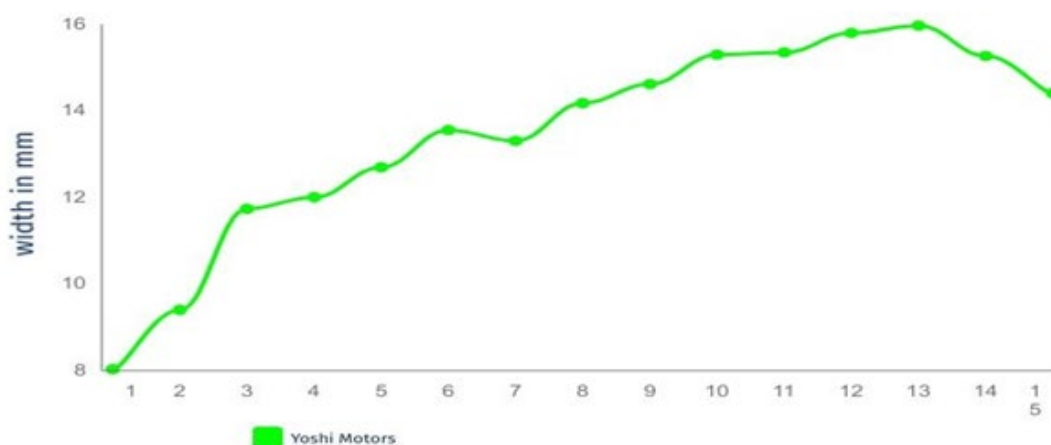


**Figure 23:** Graph is plotted between layers and their respective widths in Double pulse welding.

After deposition of every layer, the wall thickness, height of the welded layer at both the ends and middle are observed and noted as below (TABLE 3) Graphs are plotted between layers and their

respective heights (Fig. 22) and between layers and respective widths (Fig. 23) in pulse welding. Increase and decrease in width is observed because of the bulge on the top most layer.

**TABLE 4 - CURRENT AND VOLTAGE FOR EACH LAYER - DOUBLE PULSE**

Layer	Current (A)	Voltage (V)
Layer 1	119	19.3
Layer 2	121	18.8
Layer 3	118	19.5
Layer 4	121	19.0
Layer 5	119	19.9
Layer 6	119	19.7
Layer 7	117	19.5
Layer 8	117	19.8
Layer 9	116	19.3
Layer 10	114	20.0
Layer 11	115	19.2
Layer 12	113	19.7
Layer 13	117	19.6
Layer 14	115	20.3



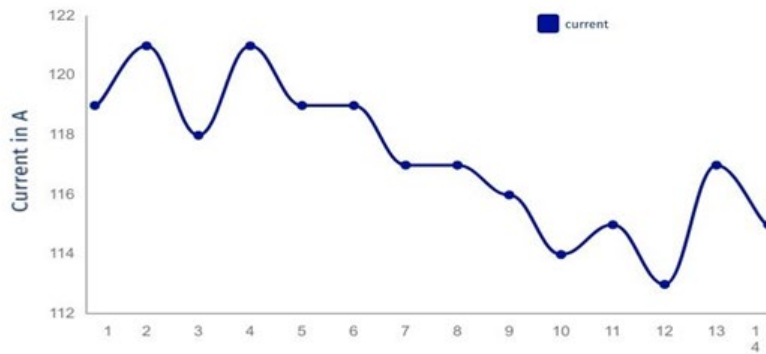


**Figure 24:** Graph is plotted between layers and their respective input current in ampere in double pulse welding.

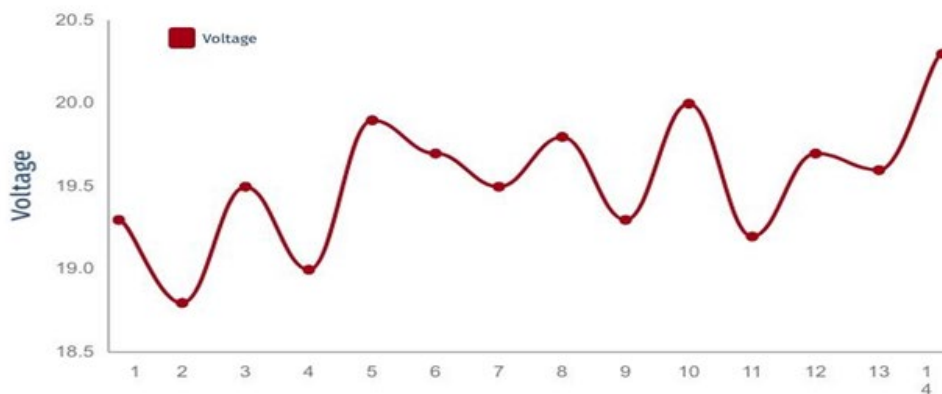


**Figure 25:** Graph is plotted between layers and their respective input voltage in volt double pulse welding.

Fluctuation in current is more in double pulse when compared pulse as the current is pulsed twice.

### Testing For Microstructures

Microstructure is a very small-scale structure of a metal. It is defined as the structure of a surface of material as revealed by an optical microscope above 25 $\times$  magnification. The microstructure of a metal can strongly influences physical properties such as strength, toughness, ductility, hardness, corrosion resistance, high or low temperature behavior or wear resistance. These properties in turn govern the application of these materials in industrial practices. Influence of microstructure on the mechanical and physical properties of a metal is primarily governed by the different defects present or absent of the

structure. Primary defects are the pores. Even if those pores play a very important role in defining the characteristics of a metal, so does its composition.

### Microstructure in the Sample Welded Using Pulse Mig Welding

The defect shown in Fig. 26 is porosity. This happens when the shielding gas gets trapped within the component and forms a bubble. This defect is almost impossible to rectify. The grain structure of the welded material using Pulse MIG method is observed. Pores with diameter 24.66 $\mu\text{m}$ , 27.66 $\mu\text{m}$  and 45.99 $\mu\text{m}$  being the larger pore has been observed in the sample welded using GMAW-P (as shown in Fig. 26).

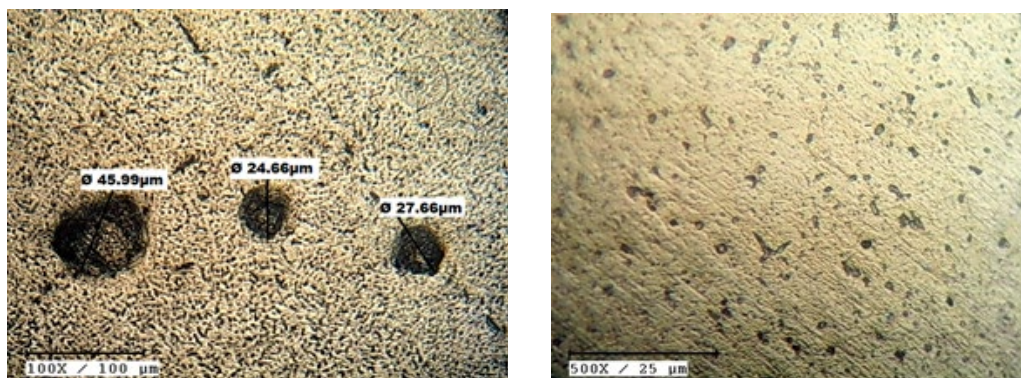


**Figure 26:** Microstructure in sample welded using pulse in a) 100X, b) 500X

## B. MICROSTRUCTURE IN THE SAMPLE WELDED USING DOUBLE PULSE MIG WELDING

Pores are found in this method too but the defect rate is very low i.e. the number of pores and slags found are less. The pores have a diameter of 16.87 $\mu\text{m}$  and 21.667 $\mu\text{m}$  being the larger pore size shown in Fig. 27.

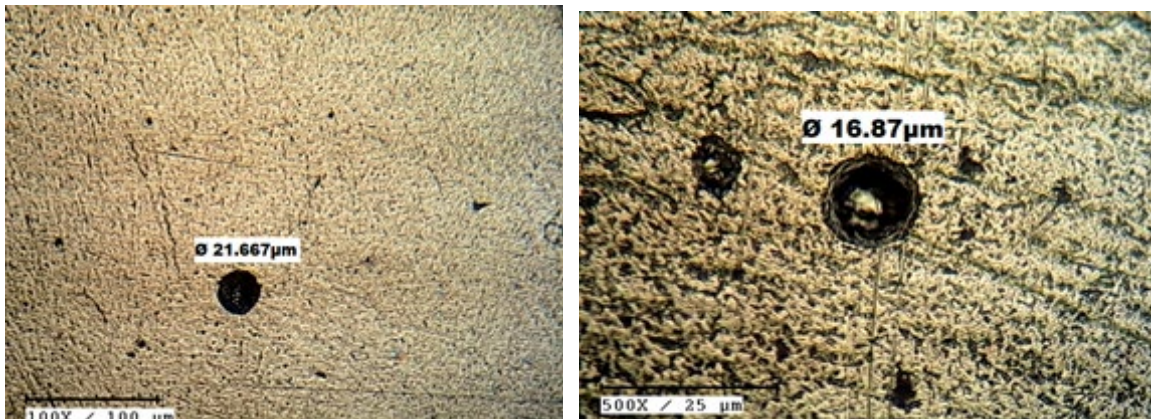


**Figure 27:** Microstructure in Sample Welded Using Double Pulse in a) 100X, b) 500X

### Conclusion

Some defects are observed in both Pulse and Double Pulse Welding. Bead formation and continuity looks better on Double Pulse Welding when compared to Pulse MIG welding. Pores formed due to the shielding gas are found in a larger number in pulse than Double pulse. Microstructure proves the excellent formation of grain structure in both types. Pores and other defects may be found in the component but still the strength and durability remain unaffected. When compared to each other Double pulse welding has a better structure and formability. The diameter of the largest pore observed in GMAW-P is 45.99 $\mu\text{m}$  and the diameter of largest pore observed in GMAW-DP is 21.667 $\mu\text{m}$ . Comparatively, the component welded by double pulse welding has a larger number of pores and is weaker than the component welded by double pulse welding.

### Future Scope

Wire Arc additive Manufacturing can be used for fabricating customized products on a regular basis so that new and personal products can be manufactured and explored. Manufacturing processes can be reduced so the availability of good quality products at low prices can be increased. The freedom in the geometric design will lead to unimaginable structural changes in the aerospace industry. The less heavy component with equivalent strength can bring changes in the Automobile industry as well. The use of Additive manufacturing has been increasing all over the globe, it will have a great use in aerospace, medical, transportation, energy, consumer services in the future [1-25]

### References

1. Mehnen, J., Ding, J., Lockett, H., & Kazanas, P. (2014). Design study for wire and arc additive manufacture. *International Journal of Product Development* 20, 19(1-3), 2-20.
2. Martina, F.: Wire + arc additive vs. from solid (2015)
3. Williams, S. W., Martina, F., Addison, A. C., Ding, J., Pardal, G., & Colegrove, P. (2016). Wire+ arc additive manufacturing. *Materials science and technology*, 32(7), 641-647.
4. Ding, J., Martina, F., & Williams, S. (2015). Production of large metallic components by additive manufacture—issues and achievements. *Welding Engineering and Laser Processing centre, Cranfield University*.
5. Standard, A. S. T. M. (2012). Standard terminology for additive manufacturing technologies. *ASTM International F2792-12a*, 1-9.
6. Oliveira, J. P., Crispim, B., Zeng, Z., Omori, T., Fernandes, F. B., & Miranda, R. M. (2019). Microstructure and mechanical properties of gas tungsten arc welded Cu-Al-Mn shape memory alloy rods. *Journal of Materials Processing Technology*, 271, 93-100.
7. Cong, B., Ding, J., & Williams, S. (2015). Effect of arc mode in cold metal transfer process on porosity of additively manufactured Al-6.3% Cu alloy. *The International Journal of Advanced Manufacturing Technology*, 76, 1593-1606.
8. Almeida, P. M., & Williams, S. (2010). Innovative process model of Ti-6Al-4V additive layer manufacturing using cold metal transfer (CMT). In *2010 International Solid Freeform Fabrication Symposium*. University of Texas at Austin.
9. Martina, F., Colegrove, P. A., Williams, S. W., & Meyer, J. (2015). Microstructure of interpass rolled wire+ arc additive manufacturing Ti-6Al-4V components. *Metallurgical and Materials Transactions A*, 46(12), 6103-6118.
10. Xie, Y., Zhang, H., & Zhou, F. (2016). Improvement in geometrical accuracy and mechanical property for arc-based additive manufacturing using metamorphic rolling mechanism. *Journal of Manufacturing Science and Engineering*, 138(11), 111002.
11. Hönnige, J. R., Colegrove, P., & Williams, S. (2017). Improvement of microstructure and mechanical properties in wire+ arc additively manufactured Ti-6Al-4V with machine hammer peening. *Procedia engineering*, 216, 8-17.
12. Hönnige, J., Colegrove, P., Prangnell, P., Ho, A., & Williams, S. (2018). The effect of thermal history on microstructural evolution, cold-work refinement and  $\alpha/\beta$  growth in Ti-6Al-4V wire+ arc AM. *arXiv preprint arXiv:1811.02903*.
13. Sun, R., Li, L., Zhu, Y., Guo, W., Peng, P., Cong, B., ... &

- 
- Liu, L. (2018). Microstructure, residual stress and tensile properties control of wire-arc additive manufactured 2319 aluminum alloy with laser shock peening. *Journal of Alloys and Compounds*, 747, 255-265.
14. Oliveira, J. P., Panton, B., Zeng, Z., Andrei, C. M., Zhou, Y., Miranda, R. M., & Fernandes, F. B. (2016). Laser joining of NiTi to Ti6Al4V using a Niobium interlayer. *Acta Materialia*, 105, 9-15.
  15. Unfried-Silgado, J., & Ramirez, A. J. (2014). Modeling and characterization of as-welded microstructure of solid solution strengthened Ni-Cr-Fe alloys resistant to ductility-dip cracking part I: Numerical modeling. *Metals and materials international*, 20, 297-305.
  16. Carter, L. N., Attallah, M. M., & Reed, R. C. (2012). Laser powder bed fabrication of nickel-base superalloys: influence of parameters; characterisation, quantification and mitigation of cracking. *Superalloys*, 2012(6), 2826-2834.
  17. Wu, B., Pan, Z., Ding, D., Cuiuri, D., Li, H., Xu, J., & Norrish, J. (2018). A review of the wire arc additive manufacturing of metals: properties, defects and quality improvement. *Journal of Manufacturing Processes*, 35, 127-139.
  18. Haden, C. V., Zeng, G., Carter III, F. M., Ruhl, C., Krick, B. A., & Harlow, D. G. (2017). Wire and arc additive manufactured steel: Tensile and wear properties. *Additive Manufacturing*, 16, 115-123.
  19. Yilmaz, O., & Uglu, A. A. (2017). Microstructure characterization of SS308LSi components manufactured by GTAW-based additive manufacturing: shaped metal deposition using pulsed current arc. *The International Journal of Advanced Manufacturing Technology*, 89, 13-25.
  20. Queguineur, A., Rückert, G., Cortial, F., & Hascoët, J. Y. (2018). Evaluation of wire arc additive manufacturing for large-sized components in naval applications. *Welding in the World*, 62(2), 259-266.
  21. Wang, L., Xue, J., & Wang, Q. (2019). Correlation between arc mode, microstructure, and mechanical properties during wire arc additive manufacturing of 316L stainless steel. *Materials Science and Engineering: A*, 751, 183-190.
  22. Fang, X., Zhang, L., Li, H., Li, C., Huang, K., & Lu, B. (2018). Microstructure evolution and mechanical behavior of 2219 aluminum alloys additively fabricated by the cold metal transfer process. *Materials*, 11(5), 812.
  23. Manikandan, N., SWAMINATHAN, G., Anirudh, R., Ranjith, S. I., Saiteja, A., & SRI, S. (2022). Comparative Study on the Microstructure Evaluation of Al-Mg (Er5356) Aluminum Alloy for Aircraft Wing Stiffener Fabricated By Wire Arc Additive Manufacturing.
  24. Yehorov, Y., da Silva, L. J., & Scotti, A. (2019). Balancing WAAM production costs and wall surface quality through parameter selection: a case study of an Al-Mg5 alloy multilayer-non-oscillated single pass wall. *Journal of Manufacturing and Materials Processing*, 3(2), 32.
  25. Grebmalai, J., & Warinsiriruk, E. (2020, October). Multi-heat input technique for aluminum WAAM using DP-GMAW process. In *AIP Conference Proceedings* (Vol. 2279, No. 1, p. 050001). AIP Publishing LLC.

**Copyright:** ©2023 Manikandan N, et al. This is an open-access article distributed under the terms of the Creative Commons Attribution License, which permits unrestricted use, distribution, and reproduction in any medium, provided the original author and source are credited.